THE JOURNAL OF PHYSICAL CHEMISTRY Letters

Letter

pubs.acs.org/JPCL

Experimental Observation of Crystal−Liquid Coexistence in Slit-Confined Nonpolar Fluids

Milena Lippmann,*[,†] Oliver H. Seeck,[†] Anita Ehnes,[†] Kim Nygård,[‡] Florian Bertram,[†] and Anca Ciobanu[†]

[†]Deutsches Elektronen-Synchrotron DESY, Notkestraße 85, 22607 Hamburg, Germany

[‡]MAX IV Laboratory, Lund University, Fontongatan 2, 22484 Lund, Sweden

ABSTRACT: Films of carbon tetrachloride (CCl_4) confined in slit geometry between two flat diamond substrates down to a few tens of Angstroms are studied by combining X-ray reflectivity with in-plane and out-of-plane X-ray scattering. The confined films form a heterogeneous structure with coexisting regions of liquid and crystalline phases. The liquid phase shows short-range ordering normal to the surfaces of the substrates. The experiments directly show the ability of the confinement to induce crystal objects, which is a long-discussed issue in the literature. The surface structure and morphology of the substrates may influence the actual realization of the crystalline phase in confinement.

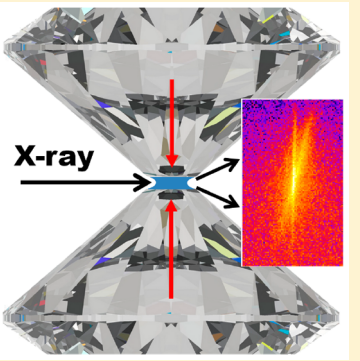

On the nanometer scale, the classical chemical and physical understanding of matter breaks down. Confinement and quantum effects dominate the nanoworld and have strong impact on reactions, phase transitions, and structure. The challenge nowadays is to understand and control the nanoworld, which is significant for the development of, for example, new catalytic, energy storage, or functional materials. Therefore, the nanosciences rapidly developed in the last decades, covering nanochemistry, nanophysics, and nanobiology. One fundamental aspect in the nanoworld is the effect of confinement on chemical and physical properties of fluids or solutions.[1,2] The molecular order of nonpolar liquids constrained to films of a few molecular diameters exhibits distinct features, which cannot be found in bulk liquids. A well-known example is the formation of molecular layering along the surface normal of the confining substrates.[3,4] Another aspect is the observation that the shear modulus and the viscosity of confined liquids are similar to those of the solid bulk phase.[5−7] The latter phenomenon is known as confinement-induced solidification and has been the subject of discussion in the literature for a long time. One suggestion is that the confinement-induced solidification is driven by crystallization of the confined film.[5,8] Other investigations suppose that on reduction of the confining gap, the liquid continuously approaches a glassy state.[6,7] Indirect experimental probes such as the surface force apparatus (SFA) cannot deliver an unambiguous answer.[9]

Liquids can be confined inside pores[2] or in a single gap in the so-called slit geometry.[3,4] X-ray scattering techniques, in principle, are a direct way to prove the existence or absence of layering and crystal phases in confined liquids. Measurements of liquids in porous materials are relatively straightforward to perform. However, the pore walls are not accessible for X-ray surface scattering methods because of the curved geometry; thus, the structure of the solid−liquid interface in a pore is very difficult to access. X-ray experiments in slit geometry can be done with high interface sensitivity.[10−14] This is eminently important, for example, when studying tribology phenomena between two substrates.

Carbon tetrachloride (CCl_4), which has nonpolar molecules with a diameter of about 5 Å, has been confined. It is well-suited for X-ray investigations, as even at high pressure and elevated temperature, no radiation damages are observed.[15−19]

This current Letter presents unambiguous experimental evidence for crystallization of molecular liquids driven by confinement. It is the first direct experimental observation of confinement-induced crystallization of a nonpolar liquid and supports theoretical studies that entropy changes due to the constrained geometry are the driving force for crystallization. In addition, the surface structure and morphology of the substrates influence the actual realization of the crystalline phase in confinement. These findings have strong impact on the ability to control chemical reactions and physical processes in constrained environments. Moreover, it is significant for lubrication properties of the confined fluid in terms of tribology.

The X-ray scattering measurements were carried out at the synchrotron radiation sources PETRA III, at beamline P08,[20] and ESRF, beamline ID03,[21] with an X-ray energy of 18 keV and beam size of (VXH) = (5 × 50) μm^2. The reflectivity

Received: February 5, 2019
Accepted: March 22, 2019
Published: March 22, 2019

DOI: 10.1021/acs.jpclett.9b00331
J. Phys. Chem. Lett. XXXX, XXX, XXX−XXX

curves were measured with area detectors (PILATUS 100k and MAXIPIX TAA22PC, respectively). The in-plane and out-of-plane scattering was recorded with a two-dimensional (2D) XRD1621 PerkinElmer (PE) area detector located 1400 mm from the sample. Finally, as a reference, X-ray scattering from bulk CCl_4 was measured at beamline P08 using a PE area detector at an energy of 25 keV and a sample−detector distance of 564 mm.

The diamond substrates are clean with wet chemicals. The cleaning procedure and the mounting of the diamond pairs are carried out in a clean room lab under a class 2 (ISO IV) laminar flow box. Before studying the confined liquid, the closed gap without liquid has been characterized by means of reflectivity and in-plane scattering measurements. Those measurements are the reference data and are also used to ensure that the substrates are not contaminated with dust particles generating crystal diffraction peaks. The liquid is injected into the reservoir of the cell and slightly heated (3 °C above room temperature). The liquid film is created by condensation of the liquid at the colder diamond substrates. In this way, possible contaminations in the liquid are not transferred onto the substrates. The reflectivity curves and in-plane scattering of the liquid film are measured before confinement. The confined is only achieved by closing the gap between the diamonds. The experiments are performed at room temperature and at normal ambient pressure, as no sealing has been used. For each experiment, a new pair of diamond is used. The experimental data presented in this work are collected at four different beamtimes.

In the literature, the influence of the surface properties and morphology of the confining walls is usually not addressed. In theoretical and simulation studies, it is often assumed that nonpolar fluid particles interact with the perfectly smooth surface of the substrates, exhibiting hard-core or van der Waals potentials. This model works well for liquids confined between mica surfaces, which are widely used in experiments and can be prepared atomically smooth and clean.[22] However, mica has severe disadvantages due to its eminent X-ray scattering into the whole reciprocal space. In the current experiment, we use (100)-oriented diamond culets with a diameter of 200 μm, which generate almost no background up to 3.5 $Å^{-1}$. These substrates are not atomically smooth on the short-range scale (see Figure 1a,b). Nevertheless, the investigation of confined liquids with such surfaces is very useful (e.g., in the context of engineering science or tribology).

To determine the long-range flatness of the substrates, we probe the native culet surfaces with X-ray reflectivity. According to this, the long-range root-mean-square (rms) flatness was determined by analysis[23] of the reflectivity curve and is better than 7 Å over the diameter of the sample, which corresponds to 15 Å peak to peak. Complementary to the reflectivity measurements, atomic force microscopy (AFM) observations are used to characterize the substrates. AFM measurements reveal a grooved structure with depth of around 15 Å (see Figure 1b) and nonregular in-plane width distribution in the range from 100 nm down to at least 10 nm (see Figure 1a). A regular terrace structure is not observed, and the images at different scales show nearly the same pattern. The AFM measurement is sensitive to the local roughness and cannot average the surface properties over the entire sample. In summary, the results from the reflectivity measurements agree very well with the average depth of the grooves as determined from the AFM images. The long-range flatness of the substrate ensures a very well-defined nanogap over the entire sample.

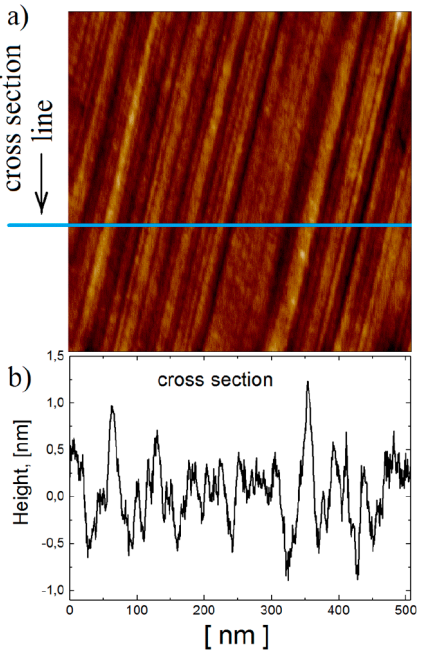

Figure 1. (a) AFM image of a 500 × 500 nm^2 area scanned in the center of the culet, and (b) the cross section of the surface at the horizontal line as indicated in Figure 1a.

The reflectivity of the confined film is sensitive to the averaged gap size (GS), which can in our case be determined from the fringes at low q-range (see Figure 2a). The samples are denoted with GS, and the number corresponds to the film thickness in Å. The reflectivity measurements at high-q_z-range are sensitive only to the molecular ordering in the vertical direction of the gap. For very large confining gaps, we are essentially probing single solid−liquid interfaces by X-ray reflectivity. Because the liquid is expected already to order at the single interface, this should show up in the high-q_z part of the reflectivity data. We exemplify the case of a wide confining gap using sample GS300. Indeed, we observe as a result of layering at a single interface a weak structure peak at the position of the first structure peak of the bulk phase. For gaps below approximately 100 Å, the molecules become affected by both confining diamond surfaces, and the ordering of the liquid is enhanced, as is clearly seen in the data of Figure 2b. Therefore, we pay attention only to samples with a GS smaller than 100 Å.

Because of the long-range flatness of the substrates and the well-defined nanogap over the entire sample, we observe layering of the liquid parallel to the interfaces, similar to the SFA experiments with atomically smooth surfaces. The fingerprint for that consists of the wide structure peaks in the reflectivity curves at $q_1 = 1.2$ $Å^{-1}$ and $q_2 = 2.3$ $Å^{-1}$[24−27] (see Figure 2b), proving the existence of a layered liquid structure. The reflectivity curves of Figure 2b, GS30, cannot be fitted,[23] assuming a constant density of the liquid or assuming layered CCl_4 molecules approximated by spheres. Instead, the positions of the liquid-layering peaks imply that the internal structure of the molecules and their ordering has to be considered. To demonstrate this point, we suggest a simple model consisting of carbon- and chlorine-rich layers. For GS30 with a total thickness of 7.2 Å, two carbon-rich layers together

DOI: 10.1021/acs.jpclett.9b00331
J. Phys. Chem. Lett. XXXX, XXX, XXX−XXX

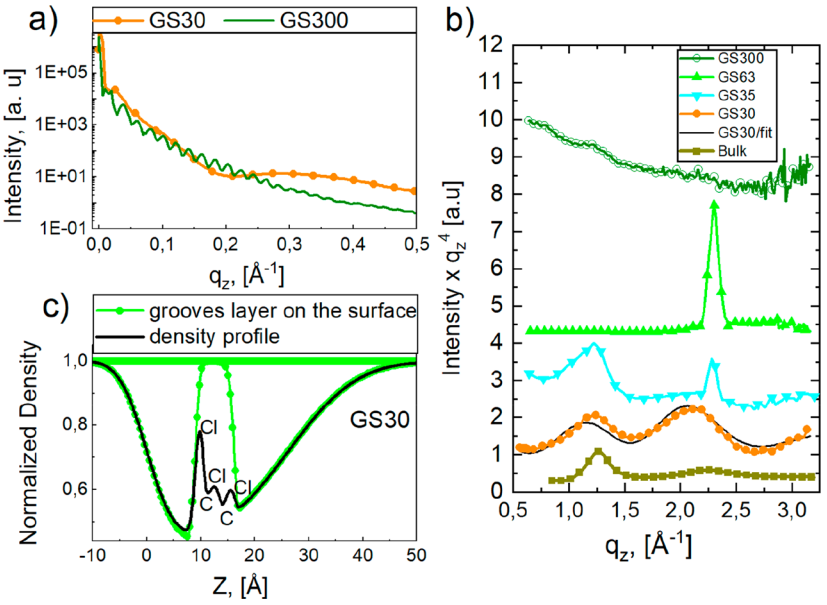

Figure 2. (a) Interference fringes on the reflectivity curve for samples GS300 and GS30 at low q-range. (b) The high-q_z part of the reflectivity curves for the given samples, multiplied by q_z^4. The curves are scaled and shifted for clarity. (c) Normalized density profile as calculated after refinement of reflectivity curve of sample GS30.

with the correspondent three chlorine-rich layers are considered (see Figure 2c). This model reproduces the main features of the measurement but leaves room for improvement as can be seen from the Figure 2b. A realistic model would include the mutual orientation of the molecules from layer to layer[17] and an accurate description of the diamond interface. Currently, such a detailed model is not available, and a better meaningful fit of the reflectivity data cannot be presented.

We want to note two observations: (1) In strong confinement, the reflectivities extend to larger q_z as compared to open gaps or large gaps. This can be seen in Figure 2b, where the reflectivity of GS300 significantly decreases with increasing q_z. The high intensity at large q_z is a direct proof of the existence of smoother interfaces than the substrates. In our model, the smooth interfaces are generated by the layer structure in the gap (see Figure 2c). This implies hypothetical buffer layers (groove layers in Figure 2c) on both sides of the diamond surface. The origin of the buffer layer could be that the liquid fills the grooves of the diamond surface or that in general a flat layered structure is favored in strong confinement. We lack a solid explanation for this behavior, but the observations are unquestionable. (2) The layer structure in the gap (Figure 2c) is slightly asymmetric due to nonidentical diamond substrates.

Nevertheless, we emphasize that the broad layering signatures, as seen in Figure 2b, are the manifestation of the liquid's short-range order in confinement[17,24−27] and therefore unmistakably prove the existence of a liquid phase in the confined CCl_4. The structure peaks in the reflectivity curve are compared with the bulk structure factor in Figure 2b. Figure 2b displays normalized X-ray reflectivity data at large q_z, multiplied by q_z^4 to account for the Fresnel reflectivity from a flat interface.[23] This standard procedure in the case of thin films is used to emphasize the structure of the film. In addition to the broad layering signatures, discussed above, narrow peaks are observed, indicating long-range order (see Figures 2b and 3a). We attribute these narrow reflections to a crystalline structure of CCl_4,[15,16] which coexists with the liquid phase.

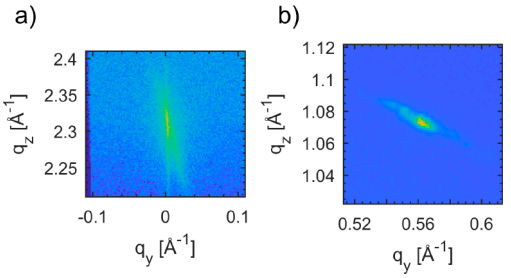

Figure 3. 2D images (in-plane and out-of-plane scattering) of different samples. Data collected from the empty gap has been subtracted. (a) 2D image of the peak observed in the reflectivity curve at $q_z \approx 2.3$ Å^{-1} of sample GS63 (cf. Figure 2b). The vertical stripe is from the specular reflected beam, and it is induced by the structure of the diamond surface and the layering. The tilted reflection is from the CCl_4 crystal structure. (b) Example of a nonspecular Bragg peak at $q \approx 1.2$ Å^{-1} of sample GS60 showing a strongly elongated elliptical shape. This image is recorded at an incident angle of 0.1°.

Moreover, the X-ray scattering data from the 2D detector (see Figure 3b) with in-plane and out-of plane information shows similar peaks with a strongly elongated elliptical shape, providing unambiguous evidence for the formation of a crystalline phase. Only a few elongated peaks are observed per sample in the 2D images, but they are present in almost all investigated samples. These reflections appear close to the q-values where the ring of the first or second bulk liquid structure peaks should be. The shape and the positions of these Bragg peaks indicate that the crystallographic planes causing the reflections are not parallel to the diamond surface. The observed reflections at $q = 1.2$ A^{-1} and $q = 2.3$ A^{-1} are in the vicinity of the strongest Bragg reflections of the monoclinic CCl_4 Phase II crystal. The reflection at $q = 1.2$ A^{-1} is also close to the strongest reflection of the cubic phase. The literature sources report that in confinement, some of the substances show peaks that do not coincide with what is known from the bulk.[28] The small amount of the observed reflections is not

DOI: 10.1021/acs.jpclett.9b00331
J. Phys. Chem. Lett. XXXX, XXX, XXX−XXX

sufficient for unambiguous identification of the CCl_4 crystal modifications.

The crystallite size is estimated from the width of the observed Bragg peaks using Scherrer's equation.[29] We note that for some of the samples, the crystallite size is larger than the film thickness (see Table 1). Tilting of the crystals with respect to the diamond surface makes the crystal size larger than the possible gap size, which can explain this result. A reasonable explanation could be that the confinement-induced crystals grow along preferred directions of the diamond surfaces (e.g., along the facets of the surface structure (cf. Figure 1a)). We do not observe a clear trend between the gap size and the crystal size. The interface structures of the diamond substrates are not commensurate with each other, and no control over the orientation of the facets on the top and bottom diamond is possible with our experimental setup at this time. We propose that the size and the orientation of the crystals are correlated with the orientation of the diamond substrates with respect to each other. The X-ray reflectivity data (see Figure 2b) show different contributions of the liquid and the crystalline phase. For example, whereas GS30 exhibits liquid and GS63 exhibits crystalline order mainly, GS35 clearly shows coexistence of the liquid and the crystalline phase. The different number of Bragg reflections of each sample could be due to different orientations of the crystallites. It should be emphasized that Bragg peaks are not observed in nonconfined thin liquid CCl_4 films on smooth surfaces[19] and have never been seen in our experiments before confinement or in wide confined samples.

Table 1. Film Thickness and Crystallite Sizes

sample	crystallite size according to Scherrer's equation, [Å]
GS30	no crystal peak is observed
GS35	70
GS60	120
GS63	62
GS300	no crystal peak is observed

At normal pressure and temperature, CCl_4 is in the liquid state,[16,18] so the thermodynamic mechanism for crystallization has to be discussed. Confined systems have very different phase diagrams as compared to the bulk.[2,18,28] This is a result of the interplay between the atomic ordering of the liquid at the interface and pure confinement effects. Theoretical works and simulation studies of confined hard-sphere systems at atomically smooth surfaces[30,31] show that changes in the entropy because of the confined geometry could drive the whole system to the crystalline state at thermodynamic state points were the bulk is still a fluid. In essence, the free volume around particles (and hence entropy) increases upon crystallization of dense hard-sphere-like fluids, with the additional packing constraints in confinement facilitating the onset of this entropy-driven phase transition. This phenomenon is known as confinement-induced freezing. However, our experiments show coexistence of the liquid and the solid phase. Possibly, the crystal growth is influenced by confinement and by the local surface morphology of the diamonds. Because we do not observe crystal phases in CCl_4 films before confinement, it is obvious that the existence of the grooves/facets itself does not result in crystallization. The crystallization is triggered by the confinement process. However, there is only little work published on confined systems with rough substrates.[32] It is shown that the ordering effects in confinement are strongly dependent on the lateral correlation between both substrates. The mutual orientation of the diamond surfaces in the current case could influence the size and the orientation of the crystals, but the morphology of single substrates is not the driving force for the crystallization, because we never observed crystallization in wide confinement. Our current understanding is that entropy is the driving force for the crystallization, whereas properties of the substrates (e.g., atomic structure, smoothness, and hydrophobicity) affect the size and the orientation of the crystals. In this sense, the confinement-induced crystallization is driven by entropy of the system, which in turn depends on the morphology and mutual orientation of the both interfaces.

To our knowledge, this is the first direct experimental observation of confinement-induced crystallization of a nonpolar liquid. Our experiments directly confirm the long-discussed consideration of Klein and Kumacheva[5] about the ability of the confinement to drive not only layering but also in-plane ordering (crystallization) of simple liquids. In the literature, the in-plane ordering is mainly understood as a continuous crystalline film created between the substrates.[5,8] Our X-ray reflectivity data evidence coexistence of liquid and crystalline phases, which excludes the existence of continuous crystalline film between the substrates. Rather, we propose that crystallites, which are tilted with respect to the diamond surfaces, grow at the facets of the surface structure from both substrates. We attribute this heterogeneous structure to the interplay between the surface morphology and the entropy changes caused by the constrained geometry.[30,31] We were, unfortunately, not able to further refine the crystal structure, because we observed only few crystal reflections, and this is not sufficient for identification of the crystal phase. However, our experiments unambiguously confirm the ability of the confinement to induce crystal objects.

Finally, we note that the experimental method developed here can also be applied beyond the heterogeneous crystal−liquid coexistence in rough confinement. The prime example is the question of how water meets extended hydrophobic interfaces,[33] which is of immense importance in fields ranging from biochemistry to materials science. Theoretical and simulation studies have shown that water exhibits large density fluctuations at extended hydrophobic interfaces, possibly because of critical drying induced by the hydrophobic interface.[34] Out-of-plane X-ray scattering experiments from water confined in narrow hydrophobic slits could unambiguously corroborate this intriguing hypothesis.[35]

AUTHOR INFORMATION

Corresponding Author

*E-mail: milena.lippmann@desy.de.

ORCID

Milena Lippmann: 0000-0001-5598-6899

Notes

The authors declare no competing financial interest.

ACKNOWLEDGMENTS

We thank Jakub Drnec for assistance with the experiment at ID03/ESRF.

REFERENCES

(1) Zeng, M.; Kim, Y.-Y.; Anduix-Canto, C.; Frontera, C.; Laundy, D.; Kapur, N.; Christenson, H. K.; Meldrum, F. C. Confinement

DOI: 10.1021/acs.jpclett.9b00331
J. Phys. Chem. Lett. XXXX, XXX, XXX−XXX

Generates Single-Crystal Sragonite Rods at Room Temperature. *Proc. Natl. Acad. Sci. U. S. A.* **2018**, *115*, 7670−7675.
(2) Huber, P. Soft Matter in Hard Confinement: Phase Transition Thermodynamics, Structure, Texture, Diffusion and Flow in Nanoporous Media. *J. Phys.: Condens. Matter* **2015**, *27*, 103102.
(3) Perret, E.; Nygård, K.; Satapathy, D. K.; Balmer, T. E.; Bunk, O.; Heuberger, M.; Friso van der Veen, J. Molecular Liquid Under Nanometer Confinement: Density Profiles Underlying Oscillatory Forces. *J. Phys.: Condens. Matter* **2010**, *22*, 235102.
(4) Seeck, O. H.; Kim, H.; Lee, D. R.; Shu, D.; Kaendler, I. D.; Basu, J. K.; Sinha, S. K. Observation of Thickness Quantization in Liquid Films Confined to Molecular Dimension. *EPL* **2002**, *60*, 376−382.
(5) Klein, J.; Kumacheva, E. Confinement-Induced Phase Transitions in Simple Liquids. *Science* **1995**, *269*, 816−819.
(6) Demirel, A. L.; Granick, S. Glasslike Transition of a Confined Simple Fluid. *Phys. Rev. Lett.* **1996**, *77*, 2261−2264.
(7) Bureau, L. Nonlinear Rheology of a Nanoconfined Simple Fluid. *Phys. Rev. Lett.* **2010**, *104*, 218302.
(8) Ayappa, K. G.; Mishra, R. K. Freezing of Fluids Confined Between Mica Surfaces. *J. Phys. Chem. B* **2007**, *111*, 14299−14310.
(9) Kienle, D. F.; Kuhl, T. L. Density and Phase State of a Confined Nonpolar Fluid. *Phys. Rev. Lett.* **2016**, *117*, 036101.
(10) Lippmann, M.; Ehnes, A.; Seeck, O. H. An X-ray Setup to Investigate the Atomic Order of Confined Liquids in Slit Geometry. *Rev. Sci. Instrum.* **2014**, *85*, 015106.
(11) Golan, Y.; Martin-Herranz, A.; Li, Y.; Safinya, C. R.; Israelachvili, J. Direct Observation of Shear-Induced Orientational Phase Coexistence in a Lyotropic System Using a Modified X-ray Surface Sorce Apparatus. *Phys. Rev. Lett.* **2001**, *86*, 1263−1266.
(12) Kékicheff, P.; Iss, J.; Fontaine, P.; Johner, A. Direct Measurement of Lateral Correlations Under Controlled Nanoconfinement. *Phys. Rev. Lett.* **2018**, *120*, 118001.
(13) Nygård, K.; Kjellander, R.; Sarman, S.; Chodankar, S.; Perret, E.; Buitenhuis, J.; van der Veen, J. F. Anisotropic pair correlations and structure factors of confined hard-sphere fluids: An Experimental and theoretical Study. *Phys. Rev. Lett.* **2012**, *108*, 037802.
(14) Nygård, K.; Sarman, S.; Hyltegren, K.; Chodankar, S.; Perret, E.; Buitenhuis, J.; van der Veen, J. F.; Kjellander, R. Density Fluctuations of Hard-Sphere Fluids in Narrow Confinement. *Phys. Rev. X* **2016**, *6*, 011014.
(15) Shigematsu, K.; Sugawara, A.; Takahashi, Y. Pressure-Induced Growth of Carbon Tetrachloride Solid II in Solid Ib. *Cryst. Growth Des.* **2012**, *12*, 3402−3406.
(16) Maruyama, M.; Kawabata, K.; Kuribayashi, N. Crystal Morphologies and Melting Curves of CCl_4 at Pressures up to 330 MPa. *J. Cryst. Growth* **2000**, *220*, 161−165.
(17) Rey, R. Quantitative Characterization of Orientational Order in Liquid Carbon Tetrachloride. *J. Chem. Phys.* **2007**, *126*, 164506.
(18) Kaneko, K.; Watanabe, A.; Iiyama, T.; Radhakrishan, R.; Gubbins, K. E. A Remarkable Elevation of Freezing Temperature of CCl4 in Graphitic Micropores. *J. Phys. Chem. B* **1999**, *103*, 7061−7063.
(19) Seeck, O. H.; Müller-Buschbaum, P.; Tolan, M.; Press, W. Diffuse X-ray Scattering in Specular Direction: Analysis of a Wetting film. *EPL* **1995**, *29*, 699−704.
(20) Seeck, O. H.; Deiter, C.; Pflaum, K.; Bertam, F.; Beerlink, A.; Horbach, J.; Schulte-Schrepping, H.; Franz, H.; Murphy, B. M.; Greve, M.; Magnussen, O. The High-Resolution Diffraction Beamline P08 at PETRA III. *J. Synchrotron Radiat.* **2012**, *19*, 30−38.
(21) Balmes, O.; van Rijn, R.; Wermeille, D.; Resta, A.; Petit, L.; Isern, H.; Dufrane, T.; Felici, R. The ID03 Surface Diffraction Beamline for In-Situ and Real-Time X-ray Investigations of Catalytic Reactions at Surfaces. *Catal. Today* **2009**, *145*, 220−226.
(22) Nygård, K.; Sarman, S.; Kjellander, R. Local Order Variations in Confined Hard-Sphere Fluids. *J. Chem. Phys.* **2013**, *139*, 164701.
(23) Als-Nielsen, J.; McMorrow, D. *Elements of Modern X-ray Physics*, 1st ed.; Wiley: New York, 2001.
(24) Huisman, W. J.; Peters, J. F.; Zwanenburg, M. J.; de Vries, S. A.; Derry, T. E.; Abernathy, D.; van der Veen, J. F. Layering of a Liquid Metal in Contact With a Hard Wall. *Nature* **1997**, *390*, 379−381.
(25) Mezger, M.; Roth, R.; Schröder, H.; Reichert, P.; Pontoni, D.; Reichert, H. Solid-Liquid Interfaces of Ionic Liquid Solutions-Interfacial Layering and Bulk Correlations. *J. Chem. Phys.* **2015**, *142*, 164707.
(26) Chattopadhyay, S.; Uysal, A.; Stripe, B.; Ehrlich, S.; Karapetrova, E. A.; Dutta, P. Surface Order in Cold Liquids: X-ray Reflectivity Studies of Dielectric Liquids and Comparison to Liquid Metals. *Phys. Rev. B: Condens. Matter Mater. Phys.* **2010**, *81*, 184206.
(27) DiMasi, E.; Tostmann, H.; Ocko, B. M.; Pershan, P. S.; Deutsch, M. X-ray Reflectivity Study of Temperature-Dependent Surface Layering in Liquid Hg. *Phys. Rev. B: Condens. Matter Mater. Phys.* **1998**, *58*, R13419−R13422.
(28) Christenson, H. Confinement Effects on Freezing and Melting. *J. Phys.: Condens. Matter* **2001**, *13*, R95−R133.
(29) Warren, B. E. *X-Ray Diffraction*; Addison-Wesley Publishing Co.: London, 1969.
(30) Schmidt, M.; Löwen, H. Freezing Between Two and Three Dimensions. *Phys. Rev. Lett.* **1996**, *76*, 4552−4555.
(31) Fortini, A.; Dijkstra, M. Phase Behaviour of Hard Spheres Confined Between Parallel Hard Plates: Manipulation of Colloidal Crystal Structures by Confinement. *J. Phys.: Condens. Matter* **2006**, *18*, L371−L378.
(32) Terrón-Mejia, K. A.; López-Rendón, R.; Gama Goicochea, A. Mesoscopic Modeling of Structural and Thermodynamic Properties of Fluids Confined by Rough Surfaces. *Phys. Chem. Chem. Phys.* **2015**, *17*, 26403−26416.
(33) Chandler, D. Interfaces and the Driving Force of Hydrophobic Assembly. *Nature* **2005**, *437*, 640−647.
(34) Evans, R.; Wilding, N. B. Quantifying Density Fluctuations in Water at a Hydrophobic Surface: Evidence for Critical Drying. *Phys. Rev. Lett.* **2015**, *115*, 016103.
(35) Nygård, K. Local Structure and Density Fluctuations in Confined Fluids. *Curr. Opin. Colloid Interface Sci.* **2016**, *22*, 30−34.

DOI: 10.1021/acs.jpclett.9b00331
J. Phys. Chem. Lett. XXXX, XXX, XXX−XXX